# An Adaptive Wavelet-Based Watermarking Using Shift-Orthogonal Finite-Length Sequences

Shuhong Li Qiaorong Zhang Yadong Zhang
College of Information, Henan Uinversity of Finance and Economics
No. 80, WenHua Road, Zhengzhou, Henan, 450002 P.R.China
Tel: +86-371-63752670

*Abstract:* - This paper presents an adaptive wavelet-based image-watermarking scheme embedding shift-orthogonal finite-length sequences. This sequence has the characteristics of shift-orthogonality and mean 0, variance 1. The security of this sequence is higher than pseudo random sequence because of the parameters used to generate the sequence. Watermark embedding is based on the characteristics of the human visual system (HVS). In the process of watermark detection the normalized correlation function is used. The experimental results show that the proposed watermarking scheme is perceptual invisible and robust against attacks such as JPEG compression， additive noise, filtering and cropping.

*Key-Word:* - Image watermarking, Wavelet transform, Shift-orthogonal finite-length sequences, Correlation detection, HVS model.

## 1. Introduction

With the rapid growth of Internet and the development of digital multimedia technologies, the demand for network distribution of images and video pictures has increased dramatically in the past decade. Although digital data has been shown to have many advantages over analog data, one of the potential problems on handling the digital data is that it can be easily duplicated. Thus, the importance of copyright protection becomes very crucial. As a solution to this problem, various digital watermarking techniques have been investigated to address the issue of ownership verification.

In general, digital watermarking can be performed in spatial domain or transform domain, where the properties of the underlying transform domain can be exploited. Previous works on digital image watermarking in spatial domain utilized the modified least significant bit of some pixels in an image. This scheme is fast and straightforward. Cox *et al.* [1] proposed a watermarking technique by embedding the watermark in the large discrete cosine transform coefficients using the concept of spread spectrum communication. Xia *et al.* [2] introduced a new multi-resolution watermarking method based on the discrete wavelet transform. The watermark is embedded to the large wavelet coefficients at high and middle frequency bands of the discrete wavelet transform of an image.

To the aim of effectively selecting the image information that can be removed without degrading subjective image quality, theoretical models of the human visual system (HVS) have been deeply studied. Similarly, it is today widely accepted that robust image watermarking techniques should largely exploit the characteristics of the HVS, for more effectively hiding a robust watermark [3],[4],[5].

In this paper, we present an image watermarking method using shift-orthogonal finite-length sequences as watermarks in the wavelet transform domain. The watermark is embedded into middle frequency wavelet coefficients based on the models of the HVS [3]. We compare our experimental results with the results of different watermark sequences. In [3], the watermark is pseudo random binary sequences, which is embedded into high frequency wavelet coefficients.

The paper is organized as follows. In Section 2, we introduce the proposed adaptive watermark embedding method, which includes the HVS model in wavelet domain and the watermark, the self-orthogonal finite-length sequences. The watermark detection is introduced in Section 3. In Section 4 we provide experimental results demonstrating the high robustness of the approach to JPEG compression, additive noise, filtering and cropping. Finally, concluding remarks are provided in Section 5.

## 2. Watermarking Embedding

In this section, we explain how a shift-orthogonal finite-length watermark is embedded in the DWT domain based on the HVS model.

### 2.1 Shift-orthogonal Finite-Length Sequences

The watermarks in this paper are two-dimension shift-orthogonal finite-length sequences. First we introduce one-dimension shift-orthogonal finite-length sequence [7],[8]. Then two-dimension shift-orthogonal finite-length sequence will be introduced. This sequence has good aperiodic correlation and a lot of varieties.

A sequence $\{a_{M,l,i}; i=0,1,\cdots,M-1\}$ has length $M$ and distinct number $l$, whose autocorrelation function is given by

$$\rho_{M,l,l,i'} = \frac{1}{M}\sum_{i=0}^{M-1} a_{M,l,i}\, a_{M,l,i-i'} = \begin{cases} 1 & ;i'=0 \\ \varepsilon_{M-1} & ;i'=\pm(M-1) \\ 0 & ;i'\neq 0,\pm(M-1). \end{cases} \quad (1)$$

The sequence is finite and aperiodic as $a_{M,l,i}=0$ for i<0 and i>M-1, whereas its autocorrelation function is also finite and aperiodic. The shift-end value $\varepsilon_{M-1}$ at left and right takes the smaller magnitude for the larger length M. The shifted sequences $\{a_{M,l,i-n}; n=0,1,\cdots,M-2\}$ satisfy the following orthogonality,

$$\frac{1}{M}\sum_{i=0}^{M-1} a_{M,l,i}\, a_{M,l,i-n} = 0, \quad n=0,1,\cdots,M-2. \quad (2)$$

Fig.1 shows the aperiodic autocorrelation function of sequence $\{a_{M,l,i}; i=0,1,\cdots,M-1\}$, whose length is $M$=32, and the shift-end value $\varepsilon_{M-1}=0.1$.

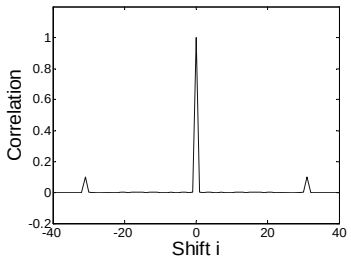


Fig.1. The aperiodic autocorrelation function.

A two-dimension shift-orthogonal finite length sequence $\{a_{M_1,M_2,L,i,j}\}$ can be produced with one-dimension shift-orthogonal finite-length sequences $\{b_{M_1,l_1,i}; i=0,1,\cdots,M_1-1\}$ and $\{b_{M_2,l_2,j}; j=0,1,\cdots,M_2-1\}$, whose sequence lengths are $M_1$ and $M_2$, sequence numbers are $l_1$ and $l_2$, ordinals are $i$ and $j$, and shift-end values are $\varepsilon_{M_1-1}$ and $\varepsilon_{M_2-1}$, respectively. The sequence $\{a_{M_1,M_2,L,i,j}\}$ and its aperiodic autocorrelation function are given by

$$a_{M_1,M_2,L,i,j} = b_{M_1,l_1,i}\, b_{M_2,l_2,j} \quad (3)$$

$$\rho_{M_1,M_2,L,L,i',j'} = \frac{1}{M_1M_2}\sum_{i=0}^{M_1-1}\sum_{j=0}^{M_2-1} a_{M_1,M_2,L,i,j}\, a_{M_1,M_2,L,i-i',j-j'} = \begin{cases} 1 & ;i'=j'=0 \\ \varepsilon_{M_1-1} & ;i'=\pm(M_1-1), j'=0 \\ \varepsilon_{M_2-1} & ;i'=0, j'=\pm(M_2-1) \\ \varepsilon_{M_1-1}\varepsilon_{M_2-1} & ;i'=\pm(M_1-1), j'=\pm(M_2-1) \\ 0 & ;otherwise. \end{cases} \quad (4)$$

Fig.2 shows the aperiodic autocorrelation function of two-dimension shift-orthogonal finite length sequence with $M_1$=$M_2$=32, and the shift-end value $\varepsilon_{M_1-1}=\varepsilon_{M_2-1}=0.1$.

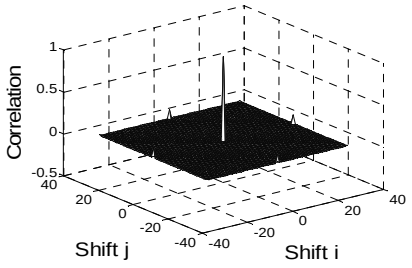


Fig.2 The aperiodic autocorrelation function of sequence

At the same time this sequence has the

characteristics of mean 0, variance $\sigma^2 = 1$. So in the experiment we compare the performance of using this sequence and pseudo random sequence with same mean and variance, which is generated by pseudo random generator.

## 2.2 Watermark Embedding

The image to be watermarked is first decomposed through DWT in four levels: let us call the sub-band $I_l^\theta$ at resolution level $l = 0,1,2,3$ and with orientation $\theta \in \{0,1,2,3\}$ (see Fig.3). The watermark, shift-orthogonal finite-length real sequence $a_{M_1,M_2,L,i,j}$, is inserted by modifying the wavelet coefficients belonging to the two detail bands at level 2, i.e., $I_1^2$ and $I_1^0$. The choice embedding the watermark only into the middle frequency sub-bands is motivated by experimental tests, as the one offering the best compromise between robustness and invisibility.

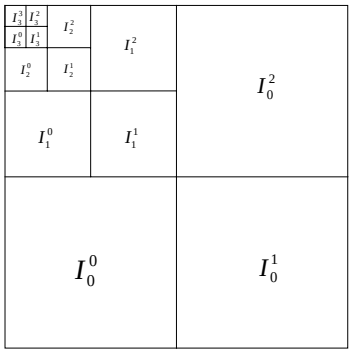


Fig. 3 Wavelet decomposition of an image in four resolution levels

The watermarks are embedded as follows:

$$\hat{I}_1^\theta(i,j) = I_1^\theta(i,j) + \alpha w_1^\theta(i,j) x^\theta(i,j) \qquad (5)$$

where $\alpha$ is a global parameter accounting for watermark strength, $w_1^\theta(i,j)$ is a weighing function considering the local sensitivity of the image to noise and $x^\theta(i,j)$ is the two-dimensional sequence $a_{M_1,M_2,L,i,j}$. This weighing function makes use of the masking characteristics of the HVS, which is decided by

$$w_1^\theta(i,j) = q_1^\theta(i,j)/2 \qquad (6)$$

where $q_1^\theta(i,j)$ is the quantization step for a DWT coefficient at sub-band $I_1^\theta(i,j)$. We assume that disturbs having value lower than $q_l^\theta(i,j)/2$ at sub-band $I_1^\theta(i,j)$ are not to be perceivable.

Based on the characteristics of the human eyes, the quantization step of each coefficient is computed as the product of three terms

$$q_l^\theta(i,j) = \Theta(l,\theta)\Lambda(l,i,j)\Xi(l,i,j)^{0.2} \quad . \qquad (7)$$

where $\Theta(l,\theta)$ is a different constant for different sub-band, which is defined by

$$\Theta(l,\theta) = \begin{Bmatrix} \sqrt{2}, & if\ \theta = 1 \\ 1, & otherwise \end{Bmatrix} \cdot \begin{Bmatrix} 1.00, & if\ l=0 \\ 0.32, & if\ l=1 \\ 0.16, & if\ l=2 \\ 0.10, & if\ l=3 \end{Bmatrix}. \qquad (8)$$

The second term takes into account the local brightness based on the gray level values of the low pass version of the image. It is computed in the following way:

$$\Lambda(l,i,j) = 1 + L(l,i,j) \qquad (9)$$

where

$$L(l,i,j) = \frac{1}{256} I_3^3\left(1 + \left\lfloor \frac{i}{2^{3-l}} \right\rfloor, 1 + \left\lfloor \frac{j}{2^{3-l}} \right\rfloor\right). \qquad (10)$$

Finally, the third term

$$\Xi(l,i,j) = \sum_{k=0}^{3-l} \frac{1}{16^k} \sum_{\theta=0}^{2} \sum_{x=0}^{1} \sum_{y=0}^{1} \left[ I_{k+l}^\theta\left(y + \frac{i}{2^k}, x + \frac{j}{2^k}\right)\right]^2 \cdot Var\left\{ I_3^3\left(1 + y + \frac{i}{2^{3-l}}, 1 + x + \frac{j}{2^{3-l}}\right)\right\}_{\substack{x=0,1 \\ y=0,1}} \qquad (11)$$

gives a measure of texture activity in the neighborhood of the pixel.

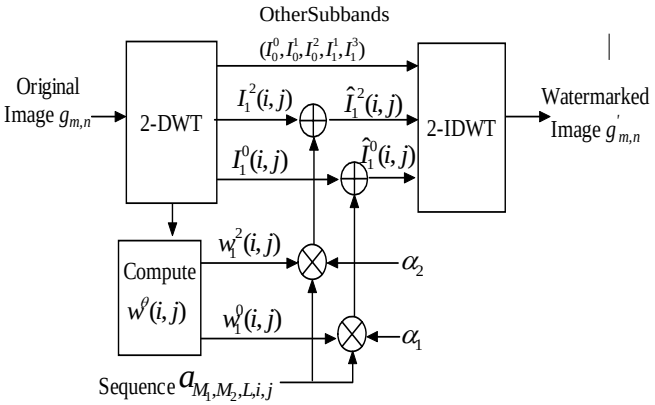


Fig.4. The diagram of watermark embedding

Fig.4 gives the block diagram of watermark embedding, in which for different sub-band $I_1^2$ and

$I_1^0$ the parameter $\alpha$ can be dissimilar considering the characteristic of them.

## 3. Watermark Detection

The block diagram of watermark detection is shown in fig.5. In the process of watermark detection the original image is needed, then we can determine whether the watermark is present or not by the normalized correlation operation between the original watermark *X* and the extracted watermark *X**, which is approximately substituted by the difference

$$\tilde{I}_1^{\theta}(i,j) - I_1^{\theta}(i,j) = \alpha \hat{w}_1^{\theta}(i,j) X^*, \qquad (13)$$

where $I_1^{\theta}(i,j)$ and $\tilde{I}_1^{\theta}(i,j)$ respectively corresponding to sub-band of the original image and the received watermarked image, which is transmitted though the channel and probably attacked by JPEG compression, filtering and so on.

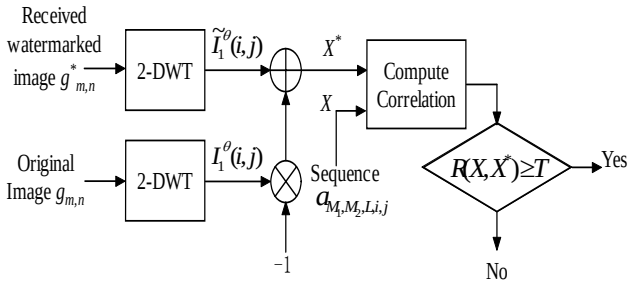


Fig.5 The block diagram of watermark detection

The normalized correlation function is defined by

$$R(X, X^*) = \frac{(X - \overline{X})(X^* - \overline{X}^*)}{\sqrt{(X - \overline{X})^2}\sqrt{(X^* - \overline{X}^*)^2}} \qquad (14)$$

and the decision is

$$R(X, X^*) < T \Rightarrow \text{watermark is not present}$$
$$R(X, X^*) \geq T \Rightarrow \text{watermark is present}$$

where the threshold *T* is evaluated by experiments. We use 10000 two-dimensional shift-orthogonal finite length sequences (not including the embedded one) and 1000 pseudo random sequences to compute the cross-correlation function with the extracted watermark from the standard test image Lena, Baboon, Cameraman and Peppers. The maximum peak value of these cross-correlation functions is 0.22, then the threshold is set to 0.30.

Because the watermark is embedded in the sub-band $I_1^2$ and $I_1^0$, the detection is successful if only one of the correlation peak values exceed the threshold.

## 4.Simulation Results and Discussion

We have performed experiments with the test images Lena, Baboon, Cameraman and Peppers of size 256×256 and the intensity levels of 8 bits. All the test images are shown in Fig.6. The watermark, two-dimension shift-orthogonal finite length sequences $\{a_{M_1,M_2,L,i,j}\}$ with $M_1$=$M_2$=32, $\varepsilon_{M_1-1}$=$\varepsilon_{M_2-1}$=-0.01. For simplicity, let the parameters $\alpha_1 = \alpha_2 = 0.1$ to ensure a good compromise of high PSNR and invisibility. The threshold of correlation detection is set up to *T*=0.3.

Fig.6 The test images are respectively Lena, Baboon, Cameraman and Peppers of size 256×256.

The PSNR and detection response of the correlation between the original images and the watermarked images are shown in Table.1. Our sequence is the shift-orthogonal finite-length sequence, and the pseudo random sequence is generated by pseudo random generator, which is real number sequence with mean 0 and variance 1. From Table.1, we can see that most of results for these sequences are similar, but performance of our sequence is a little better than that of pseudo random sequence.

Table.1 Results of the test images using different sequences

| Images | sequence | PSNR (dB) | Detection response |
|---|---|---|---|
| Lena | Our sequence | 44.77 | 0.8607 |
| | Pseudo random sequence | 44.52 | 0.8534 |
| Baboon | Our sequence | 44.21 | 0.9508 |
| | Pseudo random sequence | 44.08 | 0.9426 |
| Camera-man | Our sequence | 47.03 | 0.8511 |
| | Pseudo random sequence | 45.99 | 0.8014 |
| Peppers | Our sequence | 42.49 | 0.8723 |
| | Pseudo random sequence | 42.13 | 0.8921 |

In order to evaluate the robustness of our scheme against unintentional and intentional attacks, we test the watermarked image with JPEG compression, additive noise, filtering and cropping attacks. For simplicity, only the results of images Lena are given.

### 4.1 JPEG Compression

JPEG is a widely used compression format and the watermark should be resistant to this distortion.

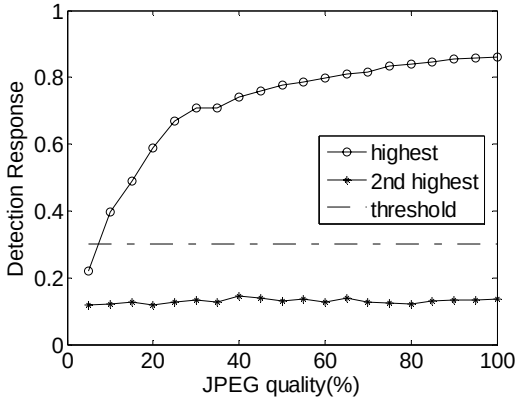


Fig.7 Detection response after JPEG compression with different quality factor.

As shown in Fig.7, with the decreasing of the quality of the JPEG compressed image, the detection response of correlation also decreases. The watermark can be detected until the quality factor is as low as 5%, although the image is severely distorted. Moreover when the quality factor is 5%, the detection response is also higher than the second highest peak value.

### 4.2 Adding Noise

Noise appears commonly in image processing and transmission. In this experiment, we add white Gaussian noise and salt and pepper noise into the watermarked image. The simulation results are shown in Fig.8 and Fig.9.

Fig.8 is the detection response of watermarked image attacked by the white Gaussian noise, where the standard deviation of noise is varied from 5% to 15% of the peak intensity 255. Fig.9 is the detection response of watermarked image attacked by the salt and pepper noise, where the density of noise to bring the intensity of pixels to 255 or 0 is varied from 1% to 10% of the size 256×256.

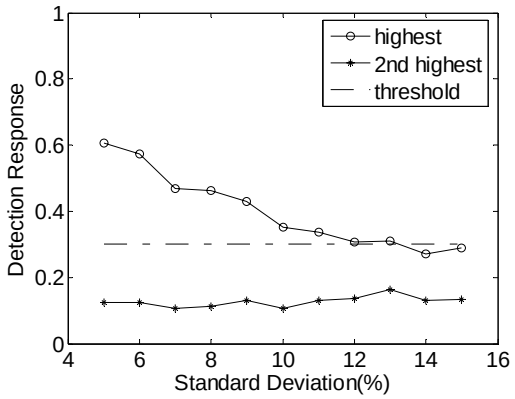


Fig.8 Detection response of white Gaussian noise attacks.

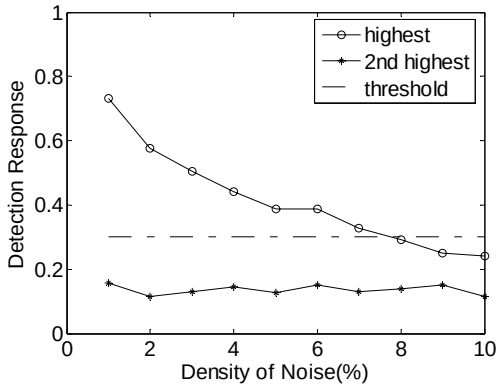


Fig.9 Detection response of salt and pepper noise attacks.

### 4.3 Filtering

Filtering is one of the common image processing. The watermarked image is filtered with 3×3 linear mean filtering and 3×3 median filtering. The results are

shown in Table 2, the PSNR is computed by original image and the watermarked image attacked by filtering. We can see the peak value of the correlation detector go beyond the threshold remarkably.

Table.2. Results of filtering attacks.

| Type of Filtering | PSNR (dB) | Detection Response |
|---|---|---|
| 3×3 linear mean filtering | 30.38 | 0.6192 |
| 3×3 median filtering | 28.59 | 0.5724 |

### 4.4 Cropping

Cropping is an important attack of geometric distortion. The watermarked image is cropped in the center by different sizes: 32×32, 64×64 and 128×128. The PSNR and detection response after cropping attacks are shown in Table.3.

Table.3 Results of cropping attacks.

| Size of Cropping | PSNR (dB) | Detection Response |
|---|---|---|
| 128×128 | 11.77 | 0.3134 |
| 64×64 | 18.25 | 0.5547 |
| 32×32 | 23.84 | 0.5989 |

## 5. Conclusion

In this article, an adaptive image watermarking scheme in wavelet transform domain has been proposed. Because of using the shift-orthogonal finite length sequences as the watermarks, the security is higher than using pseudo random sequences generated by pseudo random generator. The experimental results demonstrate that the proposed method is highly robust to JPEG compression, additive noise, filtering and cropping attacks.

**Acknowledgement**

This work is supported by Science Technology Project of Henan Province of China under Grant No.0624260019 and No.072102210001, and Natural Science Foundation of Department of Education of Henan Province of China under Grant No.2004922081.

**References:**

[1] I. J. Cox, J. Kilian, F. T. Leighton, and T. Shamoon, Secure spread spectrum watermarking for multimedia, *IEEE Trans. on Image Processing*, 6, Dec.1997, pp.1673-1687.

[2] Xia.X.-G., Boncelet.C.G., Arce, G.R. A Multi-resolution Watermark for Digital Images. *Proceeding of the IEEE International Conference on Image Processing ICIP97*, Santa Barbara, California (USA), Oct.1997, pp. 548-551.

[3] M. Barni, F. Bartolini, and A. Piva, "Improved wavelet-based watermarking through pixel-wise Masking," *IEEE Trans. on Image Processing*, 10, May.2001, pp.783-791.

[4] C. I. Podilchuk and W. J. Zheng, Image-adaptive watermarking using visual models, *IEEE Journal on Selected Areas in Communications*, 16, 1998, pp.525-539.

[5] C.H. Lee and H.K. Lee, Geometric attack resistant watermarking in wavelet transform domain, *Optics Express*, vol.13(4), Feb. 2005, pp.1309-1321.

[6] S.H. Li and Y. Tanada, A Robust Image Watermarking by Embedding Shift-orthogonal Finite-Length Sequences into Wavelet Domain, *WSEAS Trans. on Information Science and Application*s, vol.3(6), June 2006, pp.1028- 1035.

[7] Y. Tanada and T. Matsumoto, Real-Valued Convolutional PN Sequences and Their Application to Interference-Free Quasi-Synchronous CDMA, *Proc. of World Multi-conference on Systemics, Cybernetics and Informatics*, Vol.7, Jul.2000, pp.129-134.

[8] Y. Tanada, Shift-orthogonal Finite-Length Sequence and Its Derived Sequence, *Proc. of the First International Workshop on Sequence Design and Application for CDMA Systems*, Sept.2001, pp.65-73.